DOI:10.1111/j.1477-2574.2010.00223.x

ORIGINAL ARTICLE

Assessment of liver function in primary biliary cirrhosis using Gd-EOB-DTPA-enhanced liver MRI

Henrik Nilsson[1,2], Lennart Blomqvist[3,4], Lena Douglas[5], Anders Nordell[5] and Eduard Jonas[1,2]

[1]Department of Clinical Sciences, Karolinska Institutet, Stockholm, Sweden, [2]Division of Surgery, Danderyd Hospital, Stockholm, Sweden, [3]Department of Diagnostic Radiology, Karolinska University Hospital Solna, Stockholm, Sweden, [4]Institute for Molecular Medicine and Surgery, Karolinska Institutet, Stockholm, Sweden and [5]Department of Medical Physics, Karolinska University Hospital, Stockholm, Sweden

Abstract

Objectives: Gd-EOB-DTPA (gadolinium ethoxybenzyl diethylenetriaminepentaacetic acid) is a gadolinium-based hepatocyte-specific contrast agent for magnetic resonance imaging (MRI). The aim of this study was to determine whether the hepatic uptake and excretion of Gd-EOB-DTPA differ between patients with primary biliary cirrhosis (PBC) and healthy controls, and whether differences could be quantified.

Methods: Gd-EOB-DTPA-enhanced liver MRI was performed in 20 healthy volunteers and 12 patients with PBC. The uptake of Gd-EOB-DTPA was assessed using traditional semi-quantitative parameters (C_{max}, T_{max} and $T_{1/2}$), as well as model-free parameters derived after deconvolutional analysis (hepatic extraction fraction [HEF], input-relative blood flow [irBF] and mean transit time [MTT]). In each individual, all parameters were calculated for each liver segment and the median of the segmental values was used to define a global liver median (GLM).

Results: Although the PBC patients had relatively mild disease according to their Model for End-stage Liver Disease (MELD), Child–Pugh and Mayo risk scores, they had significantly lower HEF and shorter MTT values compared with the healthy controls. These differences significantly increased with increasing MELD and Child–Pugh scores.

Conclusions: Dynamic hepatocyte-specific contrast-enhanced MRI (DHCE-MRI) has a potential role as an imaging-based liver function test. The high spatial resolution of MRI enables hepatic function to be assessed on segmental and sub-segmental levels.

Keywords

liver function, MRI, Gd-EOB-DTPA, DHCE-MRI, primary biliary cirrhosis

Received 26 April 2010; accepted 6 July 2010

Correspondence

Henrik Nilsson, Karolinska Institutet, Department of Clinical Sciences, Danderyd Hospital, Division of Surgery, 182 88 Stockholm, Sweden. Tel: + 46 8 655 50 00. Fax: + 46 8 655 77 66. E-mail: henrik.nilsson@ki.se

Introduction

For liver surgeons, postoperative liver failure is a major concern and has become the biggest cause of postoperative mortality after liver resection.[1] The prediction of post-resection residual liver function is currently typically based on combinations of volumetric studies and crude assessments of global liver function, such as the Child–Pugh score (CPS) or indocyanine green (ICG) clearance.[2,3] A more reliable liver function test, capable of evaluating the status of the liver on a segmental level, whereby it would be possible to predict remnant liver function more accurately than with the currently available methods, would enable more judicious decision making and would probably result in lower postoperative mortality and morbidity. Furthermore, some liver diseases, such as primary sclerosing cholangitis (PSC), primary biliary cirrhosis (PBC), alcoholic liver cirrhosis and even

This paper was presented at the International Hepato-Pancreato-Biliary Association Meeting, 18–22 April 2010, Buenos Aires, Argentina.

non-alcoholic fatty liver disease (NAFLD) affect the liver in a non-homogeneous fashion. This makes the assessment of the degree of liver dysfunction difficult with currently available liver function tests (LFTs), which give a global assessment of liver function. Severe segmental or regional disease can be underdiagnosed.

A segmental liver function test requires sampling from individual liver segments using a non-invasive, well-tolerated and safe sampling method. Imaging-based sampling could fulfil these criteria. Resolution should be sufficient for accurate sampling from blood vessels, parenchyma and bile ducts. This would enable measuring of the uptake of a tracer from the bloodstream into the parenchyma and its subsequent excretion into the bile. Scintigraphic methods are currently the only imaging-based tests used clinically to assess liver uptake capacity and biliary excretory function. These methods, however, are hampered by low spatial resolution and the limited anatomic detail obtained.[4–6] This complicates the accurate placement of regions of interest (ROIs), especially in smaller structures. Computed tomography (CT) has sufficient resolution but its use is limited by radiation, especially when repetitive examinations are required. Magnetic resonance imaging (MRI) has the advantage of not using ionizing irradiation. Gadoxetic acid or Gd-EOB-DTPA (gadolinium ethoxybenzyl diethylenetriaminepentaacetic acid) (Primovist®; BayerSchering Pharma AG, Berlin, Germany) is a gadolinium chelate which is taken up by hepatocytes and excreted into the bile.[7,8] The pharmacokinetic properties of Gd-EOB-DTPA are similar to those of the 99mTc-IDA family in that hepatocellular uptake occurs through the organic anionic transport system (OATS) and subsequent biliary excretion by glutathione-S-transferase.[7] Pharmacokinetic studies show that about 50% of the administered dose of Gd-EOB-DTPA is extracted by the liver and secreted through the hepatobiliary pathway. The remaining 50% is eliminated by renal excretion.[8] Thus, hepatic uptake of Gd-EOB-DTPA and subsequent T_1-relaxation shortening are dependent on the integrity of the hepatocyte mass. Dynamic Gd-EOB-DTPA MRI has previously been used in animal models for the evaluation of hepatic function in various experimental settings, using either summary parameters or deconvolutional analysis (DA).[9–12] A method to evaluate segmental liver function, using dynamic hepatocyte-specific contrast-enhanced MRI (DHCE-MRI) with Gd-EOB-DTPA as tracer, has previously been described.[13]

Primary biliary cirrhosis is an autoimmune liver disease, characterized by the progressive destruction of intrahepatic bile ducts, resulting in cholestasis, portal inflammation and fibrosis, which eventually may lead to cirrhosis.[14] It predominates in females by a ratio of 9 : 1 and typically affects women aged 50–60 years.[15,16] Diagnosis is based on the presence of anti-mitochondrial antibodies (AMA) and the elevation of biochemical markers of cholestasis for a period of >6 months. Liver biopsy is no longer mandatory for diagnosis, but aids in the work-up of patients by excluding other causes of cholestasis.[17] Furthermore, it may give useful information on disease activity and stage. However, the disease does not affect the liver uniformly and there is a considerable risk for under-staging on single liver biopsies.[18] The natural history of the disease is variable and ranges from stable to rapidly progressive disease. Various attempts have been made to predict the clinical course of patients with PBC and several prognostic models have been developed to predict survival.[19–23] The Mayo Clinic survival model is the most widely used of these.[20,24]

The aim of this study was to compare DHCE-MRI-derived quantitative and semi-quantitative parameters in PBC patients with those in normal controls. In patients, results were also correlated with the CPS, Mayo risk score and Model for End-stage Liver Disease (MELD) score.

Materials and methods

Study subjects

Twelve patients with established diagnoses of PBC were included in the study and 20 healthy volunteers were used as controls. Informed consent was obtained from all participants prior to examination and the study was approved by the Regional Ethical Review Board. T_1-weighted DHCE-MRI, using Gd-EOB-DTPA, was performed. All subjects were instructed to fast for at least 4 hours prior to the examination. The healthy volunteers had no history of hepatobiliary disease, previous hepatobiliary surgery or alcohol abuse. For patients, relevant demographic and clinical data were documented, as well as the results of LFTs from the most recent visit documented in clinical charts. The CPS, Mayo risk score and MELD score were calculated for each patient.

MR procedure

Data were collected using an Intera 1.5 Tesla (T) scanner (Philips Medical Systems, Best, the Netherlands), with a four-channel SENSE body coil (Philips Medical Systems). The whole liver was examined using a dynamic T_1-weighted three-dimensional spoiled-gradient echo pulse sequence (repetition time/echo time/flip angle 4.1 ms/2.0 ms/10 °, field of view = 415 mm, matrix resolution 256 × 192, 40 slices, slice thickness 10 mm, SENSE factor R = 2). The volume was imaged in a single breath-hold at 41 different time-points (12 s scan time per acquired volume) and participating subjects were asked to hold their breath at the same depth during each acquisition. Three volumes were acquired pre-contrast for baseline calculations, followed by 38 volumes with a stepwise increase in sampling intervals up to a total sampling time of 90 min. The sampling density was chosen to account for the subjects' physical capacity, data acquisition limitations and test substance dynamics. A dose of 0.1 ml/kg Gd-EOB-DTPA 0.25 mmol/ml was injected into the right anterior cubital vein to coincide with the start of the fourth acquired volume. The contrast was injected using a power injector (Spectris MR Injector System; Medrad, Inc., Pittsburgh, PA, USA) at an infusion rate of 2 ml/s and was immediately followed by a bolus of 20 ml of saline (NaCl 0.9%) at the same infusion rate.

Image analysis

Image analysis and subsequent calculations were performed using in-house software written in MATLAB® (MathWorks, Inc., Novi, MI, USA). Liver response function curves were defined by placing three ROIs in the parenchyma of each liver segment (I–VIII), avoiding major blood vessels and visible bile ducts. The size of the ROI was chosen arbitrarily by the investigator. The combined relative enhancement over time of all the voxels in the three ROIs was regarded as the parenchymal response function of that segment. Segments were anatomically defined and the nomenclature adhered to as proposed by Strasberg.[25,26] Segment IV was subdivided into IVa and IVb. The input function, representing the blood supply to the liver, used in the deconvolution of the parenchymal response curves for calculation of the quantitative parameters, was defined by an ROI placed in the hilar part of the portal vein. To ensure that the input function ROI was truly representative of the portal vein over the entire acquisition period, it was adjusted manually as necessary. In all studies, the relative signal intensity in the ROIs was calculated as the logarithmic ratio:

$$C(t,\rho) = \ln\left(\frac{S(t,\rho)}{S_0(\rho)}\right), \qquad \text{[Eq. 1]}$$

where $C(t, \rho)$ is the relative tracer concentration at time t in voxel ρ, $S_0(\rho)$ is the mean image intensity in voxel ρ from the pre-contrast images (i.e. the baseline signal intensity), and $S(t, \rho)$ is the measured image intensity in voxel ρ at time t. The parameters described below were calculated in each liver segment for all participating subjects. In addition, a global liver median (GLM) for each parameter was calculated using the median value of the nine segmental parameters in each subject.

Semi-quantitative pharmacokinetic parameters

Parameters were defined as semi-quantitative when calculation did not take into account the impact of the input function (i.e. the amount of tracer in the circulating blood pool) on the resulting parenchymal enhancement-over-time curve. Maximum relative signal intensity (C_{max}) and time to maximum relative signal intensity (T_{max}) were calculated directly from the parenchymal enhancement-over-time curves. As the excretion half-time for Gd-EOB-DTPA is much longer than the time-span used in this study, $T_{1/2}$ (time to a 50% decline in signal enhancement) was calculated using a curve-fitting model, thus:

$$f = k_1 \cdot e^{(-\ln(2)t/T_{1/2})} - k_2 \cdot e^{(-\ln(2)t/TU)}, \qquad \text{[Eq. 2]}$$

where f is the fitted curve, the fitting parameters k_2 and TU describe contrast uptake, and k_1 and $T_{1/2}$ describe the liver contrast excretion. The bi-exponential function is not optimal for the liver response because, for example, it does not take into account any contribution to signal intensity from the blood pool. Therefore, the fit does not always converge if the whole response curve is included; $t = 240$ s was selected as the starting point for the fit.

Parameters derived from deconvolutional analysis: model-free parameters

Mathematically, the response function of an organ, in this case the liver, can be described as a convolution between the impulse response and the input function:

$$y(t) = h(t) \otimes x(t), \qquad \text{[Eq. 3]}$$

where $y(t)$ is the response function, $h(t)$ the impulse function, $x(t)$ the input function, and $\otimes$ denotes the mathematical convolution operator. The response function $y(t)$ (in this case the parenchymal enhancement-over-time curve) and the input function $x(t)$ can be measured, but $h(t)$ is unknown. However, with knowledge of the input and response functions, the impulse function can be estimated through deconvolution. From the impulse response function curves, several functional characteristics of the system can be derived, as has previously been described in functional MRI of the kidneys.[27,28] From the impulse response curve, the hepatic extraction fraction (HEF), input-relative blood flow (irBF) and mean transit time (MTT) were calculated. In several studies using scintigraphy to investigate liver function, HEF has been used as a measurement of hepatic extraction efficiency.[29–35] The HEF can be described as the proportion of tracer that would have been extracted by the liver if the tracer had entered into the system as a short bolus without recirculation, whereas the irBF describes the peak blood flow in an ROI relative to the peak blood flow in the input function. The calculation of the HEF and irBF has been extensively described in a previous publication.[13] The MTT describes the mean time for a unit of the studied substance to pass through the ROI, in this case exiting through either excretion into the bile ducts or vascular wash-out. The MTT is calculated as the area under the impulse response curve from peak value down to 0, divided by the peak value of the curve (equal to the irBF).

Analysis and statistical methods

Age and gender distributions were compared using the non-parametric Mann–Whitney *U*-test and the two-group proportionality test, respectively. The results of the segmental calculations and GLM were presented as summary statistics (median and range) and compared using the Mann–Whitney *U*-test. For parameters for which a significant difference in GLM between patients and controls was observed, a test for trend across ordered groups was used to assess the association between the CPS and MELD score. For these calculations, the controls were assigned dummy values of 4 for CPS, and 5 for MELD score. This is one unit less than the lowest possible score in these models. As the Mayo risk score was regarded as a continuous variable, Spearman's rank correlation was used instead, without assigning a dummy value for the controls. In the patient group, Spearman's rank correlation was also used to correlate the parameters in which a significant difference in GLM was seen, with regard to age. Likewise, using the Mann–Whitney *U*-test, the outcomes of these

parameters in the control group were compared, using gender as the independent variable. The significance threshold was set to $\alpha = 0.05$. STATA Version 10 (StataCorp LP, College Station, TX, USA) was used for statistical analyses.

Results

Patient characteristics are shown in Table 1. Patients in the PBC group were older than the controls ($P < 0.001$) and an expected female predominance was observed ($P < 0.01$). Liver disease in the patient group as a whole was mild, as can be seen in the relatively low CPS, MELD and Mayo risk scores. The results of the segmental calculations and GLMs in the PBC patients and the normal volunteer group are shown in Table 2. In a majority of segments, the segmental HEF and MTT measurements were significantly lower in PBC patients compared with normal volunteers. This was also observed for the GLM. With the exception of one segment (IVa), no significant differences in segmental results or GLM were found for irBF values. The results for the semi-quantitative parameters are shown in Table 3. No significant differences were observed in GLM for any of these parameters. In addition, the earliest T_{max} in the PBC group for all liver segments except segment I occurred as early as 120 s after injection of the tracer. This means that the relative signal intensity in these segments peaked when the intravascular bolus of the tracer passed, and that very little tracer was subsequently extracted.

Because HEF and MTT medians differed significantly between the patient and control groups in the majority of segmental values as well as in the GLM, further analyses were performed to investigate the impact of disease severity on these parameters. As Figs 1 and 2 show, MTT and HEF decreased significantly with increasing severity of liver disease as estimated by the CPS and MELD score, but not by the Mayo risk score (Fig. 3). In one patient and one control, HEF, irBF and MTT values were calculated in every voxel within the liver parenchyma of one slice to give the parametric maps presented in Fig. 4. Figure 5 shows age plotted against HEF and MTT in PBC patients. No statistically significant correlation was observed. In the control group, gender was not found to be a substantial confounder. Neither the median HEF nor the median MTT differed significantly for males and females ($P = 0.112$ and $P = 0.762$, respectively).

Discussion

This study used PBC as a disease model to evaluate a new method for liver function assessment. Although the number of patients in the study was small and the group represented patients only mildly affected by their disease, significant differences in quantitative parameters measuring hepatic uptake and transport of Gd-EOB-DTPA were found between patients and healthy controls. Furthermore, a significant trend towards a decrease in these parameters was observed as CPS and MELD score increased.

The semi-quantitative parameters were not useful in distinguishing between patients and normal volunteers. These parameters are more intuitive and easily understood than the model-free parameters. Because they are easily accessible and do not require advanced post-processing for calculation, they are often used to describe the pharmacokinetic kinetics in a system. However, results should be interpreted with caution. A high C_{max} may either indicate a virtually non-functioning parenchyma with arterialization caused by cirrhosis and a quick and high vascular peak, or may reflect the excellent extraction of tracer with a high parenchymal signal occurring later in the study. A short $T_{1/2}$ calculated from a time-enhancement curve generated by a parenchymal ROI is generally interpreted as good contrast agent excretion. However, in parenchyma with no extraction capacity, in which the signal is

Table 1 Patient characteristics

Patient no.	Sex	Age, years	MELD score	Child–Pugh score	Mayo score
1	Female	61	6	6	5.2
2	Female	75	6	5	5.1
3	Female	65	6	5	5.8
4	Female	57	6	6	4.4
5	Female	71	7	5	6.0
6	Female	65	6	5	4.8
7	Female	47	11	7	6.4
8	Female	53	6	5	4.0
9	Female	71	6	6	5.6
10	Female	63	6	5	4.1
11	Male	62	14	7	7.8
12	Female	63	7	6	6.3
Control group (n = 20)	M : F, 10 : 10	Median 33.5			

MELD, Model for End-stage Liver Disease

Table 2 Segmental and global results for the quantitative parameters

		Segment									Global
		I	II	III	IVa	IVb	V	VI	VII	VIII	
Control group	HEF, median	0.18	0.21	0.19	0.20	0.17	0.21	0.20	0.22	0.22	0.20
	HEF, min	0.13	0.13	0.14	0.13	0.09	0.13	0.11	0.14	0.14	0.14
	HEF, max	0.46	0.31	0.34	0.30	0.41	0.34	0.32	0.33	0.33	0.33
PBC group	HEF, median	0.16	0.16	0.14	0.16	0.15	0.16	0.16	0.19	0.17	0.16
	HEF, min	0.07	0.05	0.03	0.04	0.04	0.04	0.04	0.04	0.03	0.04
	HEF, max	0.30	0.30	0.30	0.30	0.22	0.29	0.24	0.22	0.36	0.30
P-value[a]		0.139	0.010	0.067	0.073	0.111	0.013	0.022	0.043	0.047	0.022
Control group	irBF, median	0.26	0.22	0.23	0.22	0.22	0.25	0.27	0.26	0.25	0.24
	irBF, min	0.14	0.17	0.14	0.17	0.15	0.20	0.19	0.19	0.17	0.19
	irBF, max	0.33	0.29	0.30	0.32	0.32	0.32	0.33	0.32	0.32	0.31
PBC group	irBF, median	0.27	0.23	0.23	0.25	0.25	0.28	0.28	0.28	0.25	0.25
	irBF, min	0.19	0.17	0.15	0.23	0.23	0.21	0.21	0.21	0.18	0.22
	irBF, max	0.32	0.30	0.30	0.36	0.38	0.40	0.40	0.31	0.36	0.36
P-value[a]		0.586	0.199	0.613	0.027	0.080	0.371	0.312	0.756	0.312	0.350
Control group	MTT, median	486	562	494	485	524	521	509	479	536	503
	MTT, min	289	316	251	261	248	307	287	325	295	299
	MTT, max	1629	1485	1642	1637	1589	1688	1519	1383	1723	1536
PBC group	MTT, median	368	351	393	369	369	379	350	399	350	363
	MTT, min	158	113	131	130	134	156	186	197	129	134
	MTT, max	817	734	1976	673	766	818	754	681	864	754
P-value[a]		0.057	0.011	0.161	0.047	0.020	0.052	0.036	0.102	0.027	0.029

[a]Mann–Whitney *U*-test
PBC, primary biliary cirrhosis; HEF, hepatic extraction fraction; irBF, input-relative blood flow; MTT, mean transit time

derived only from the intrahepatic blood pool, a short $T_{1/2}$ will be observed. Furthermore, a long $T_{1/2}$ that would generally be interpreted as representing decreased liver function may be the result of activity measured in obstructed bile ducts in a patient with normal parenchymal function.

A weakness of this study is the low number of participating subjects. This may have led to failure to detect actual differences between patients and controls for some of the parameters for which no significant differences or correlations with disease severity were found. Furthermore, traditional confounders such as age and gender were not controlled or corrected for. This would have been particularly fitting as the patient group was significantly older than the control group and the gender distribution was not proportional. It could be argued that the differences described should be attributed to these baseline differences between the groups, rather than to the diagnosis of PBC. However, no differences were found using age and gender as confounders in the patient and normal volunteer groups, respectively.

The results show large ranges for both the semi-quantitative and quantitative parameters in both patients and normal volunteers. As well as normal individual variation, motion artefacts and partial volume effects may also have influenced the results. Correction for motion artefacts using image registration algorithms before image analysis would be a logical next step in improving the method.

Another issue pertaining to quantitative dynamic MRI that deserves discussion is the extent of correlation between the measured signal intensity and the actual concentration of tracer in the ROI. The logarithmic ratio described in Eq. 1 was used to calculate relative contrast agent concentrations in the ROIs. It has been shown that the relationship between image intensity and Gd-DTPA concentration is non-linear for steady state MRI pulse sequences, such as the spoiled-gradient echo sequence used in this study.[36] However, when T_1 relaxation is within the range of 40–2600 ms, the MR signal was shown to increase approximately exponentially with shortening T_1 relaxation. All measurements were estimated to be within this range, making Eq. 1 a good approximation to relative contrast agent concentration.

The acquisition time in the current protocol is 90 min, which makes the method impractical for routine clinical use. For calculation of the DA-derived parameters, only data from the first 30 min of each dataset are required. This would allow the protocol to be shortened if only these parameters are calculated.

Table 3 Segmental and global results for the semi-quantitative parameters

		Segment									Global
		I	II	II	IVa	IVb	V	VI	VII	VIII	
Control group	C_{max}, median	0.533	0.473	0.451	0.459	0.448	0.574	0.574	0.557	0.553	0.537
	C_{max}, min	0.429	0.400	0.371	0.354	0.326	0.441	0.440	0.462	0.469	0.429
	C_{max}, max	0.661	0.600	0.621	0.625	0.618	0.711	0.680	0.642	0.663	0.625
PBC group	C_{max}, median	0.581	0.480	0.455	0.539	0.526	0.600	0.611	0.607	0.555	0.570
	C_{max}, min	0.276	0.269	0.288	0.324	0.324	0.376	0.319	0.319	0.360	0.319
	C_{max}, max	0.723	0.627	0.604	0.590	0.631	0.733	0.754	0.669	0.640	0.640
P-value[a]		0.414	0.613	0.785	0.331	0.120	0.846	0.436	0.350	0.697	0.640
Control group	T_{max}, median	1500	1950	1800	1230	1800	2100	2100	1950	2130	1950
	T_{max}, min	840	720	840	780	960	1020	1080	960	960	1080
	T_{max}, max	3000	3000	3000	5400	3300	3300	3300	3300	5400	2700
PBC group	T_{max}, median	2400	1800	2400	2250	2550	2550	2550	2700	2100	2250
	T_{max}, min	840	120	120	120	120	120	120	120	120	120
	T_{max}, max	5400	3000	5400	5400	5400	5400	4800	4800	5400	5400
P-value[a]		0.014	0.683	0.080	0.243	0.067	0.284	0.267	0.251	0.800	0.161
Control group	$T_{1/2}$, median	12 591	12 858	11 298	15 491	14 018	20 609	18 595	20 755	23 387	17 697
	$T_{1/2}$, min	2472	2439	2151	2321	1917	6222	3233	6197	6161	6161
	$T_{1/2}$, max	39 637	139 412	76 556	50 305	105 250	489 323	140 694	68 439	208 934	45 599
PBC group	$T_{1/2}$, median	13 305	15 898	9062	13 162	11 902	13 019	22 738	15 889	10 773	14 133
	$T_{1/2}$, min	3640	2367	1869	3496	2293	3262	4235	3657	3479	4704
	$T_{1/2}$, max	291 249	109 297	149 489	455 857	91 156	29 255	60 905	60 202	54 732	41 993
P-value[a]		0.567	0.815	0.628	0.477	0.960	0.027	0.508	0.565	0.043	0.414

[a]Mann–Whitney *U*-test
PBC, primary biliary cirrhosis; C_{max}, maximum signal intensity; T_{max}, time to maximum relative signal intensity; $T_{1/2}$, time to a 50% decline in signal enhancement

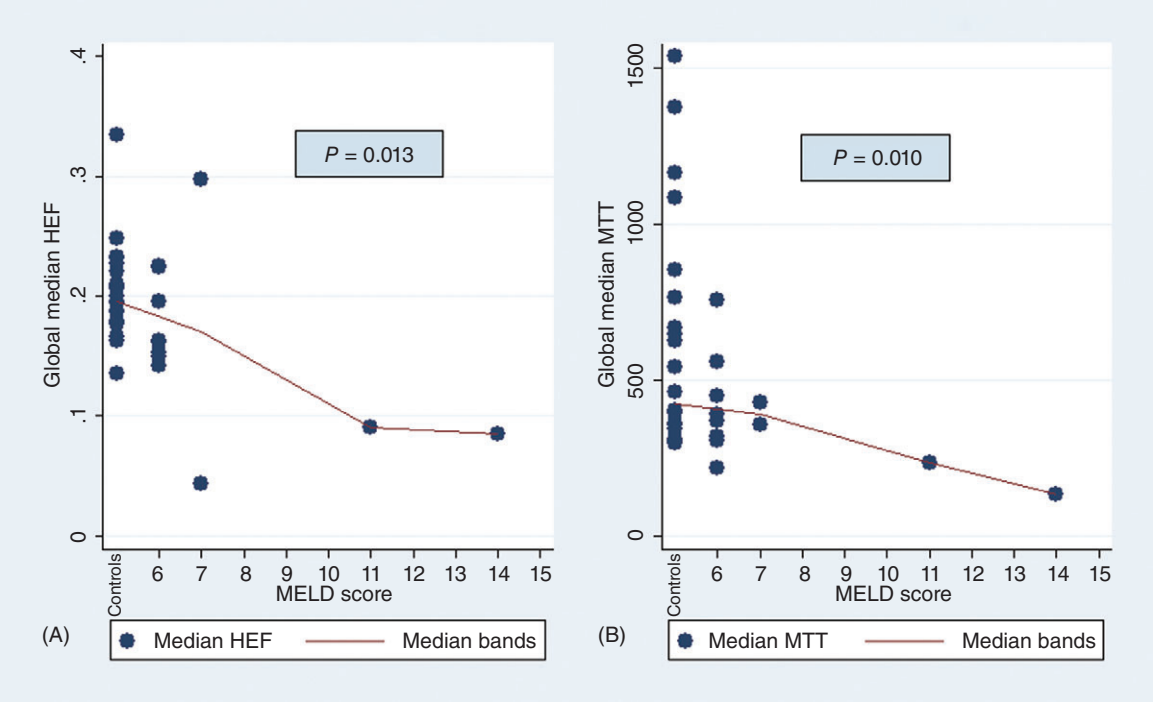

Figure 1 (A) Hepatic extraction fraction (HEF) and (B) mean transit time (MTT) plotted as a function of Model for End-stage Liver Disease (MELD) score, showing a significant trend for decreasing parameter values with increasing disease severity

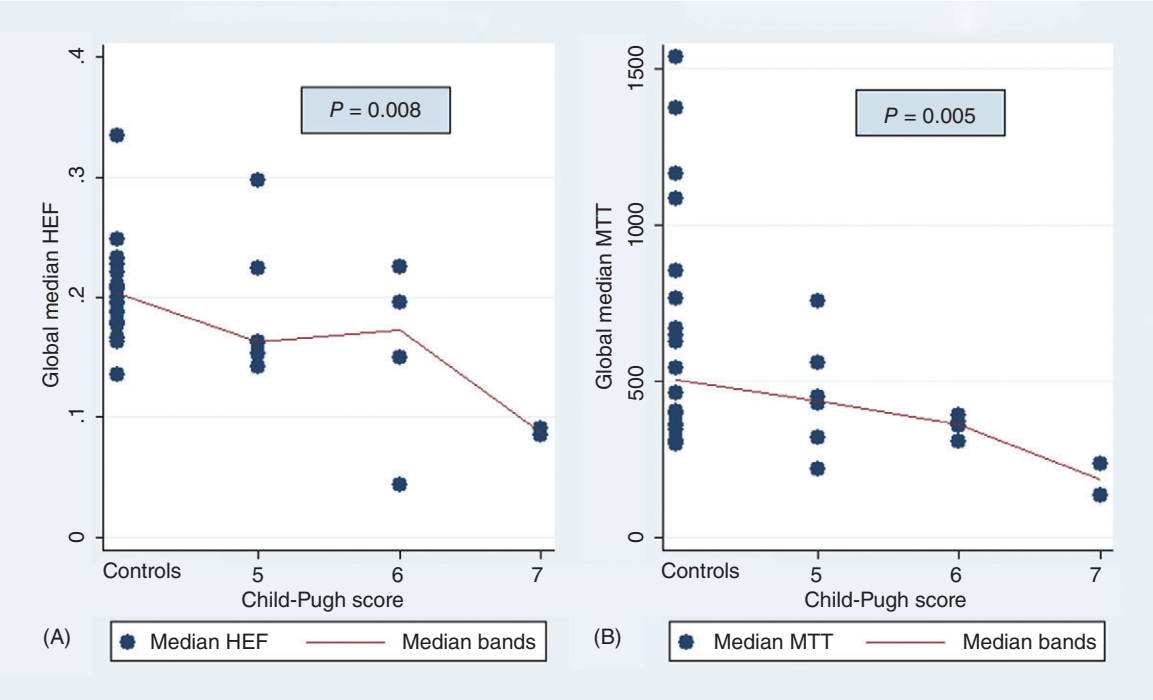

Figure 2 (A) Hepatic extraction fraction (HEF) and (B) mean transit time (MTT) plotted as a function of Child–Pugh score, showing a significant trend for decreasing parameter values with increasing disease severity

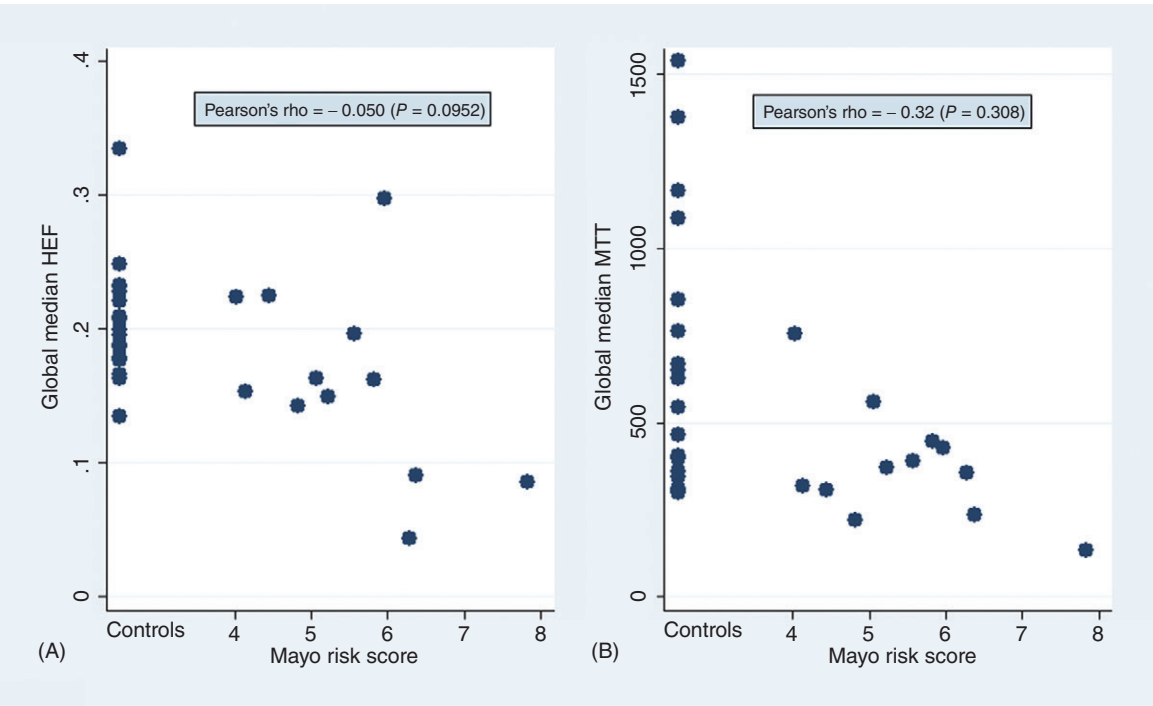

Figure 3 (A) Hepatic extraction fraction (HEF) and (B) mean transit time (MTT) plotted as a function of Mayo risk score, showing a weak negative, non-significant correlation

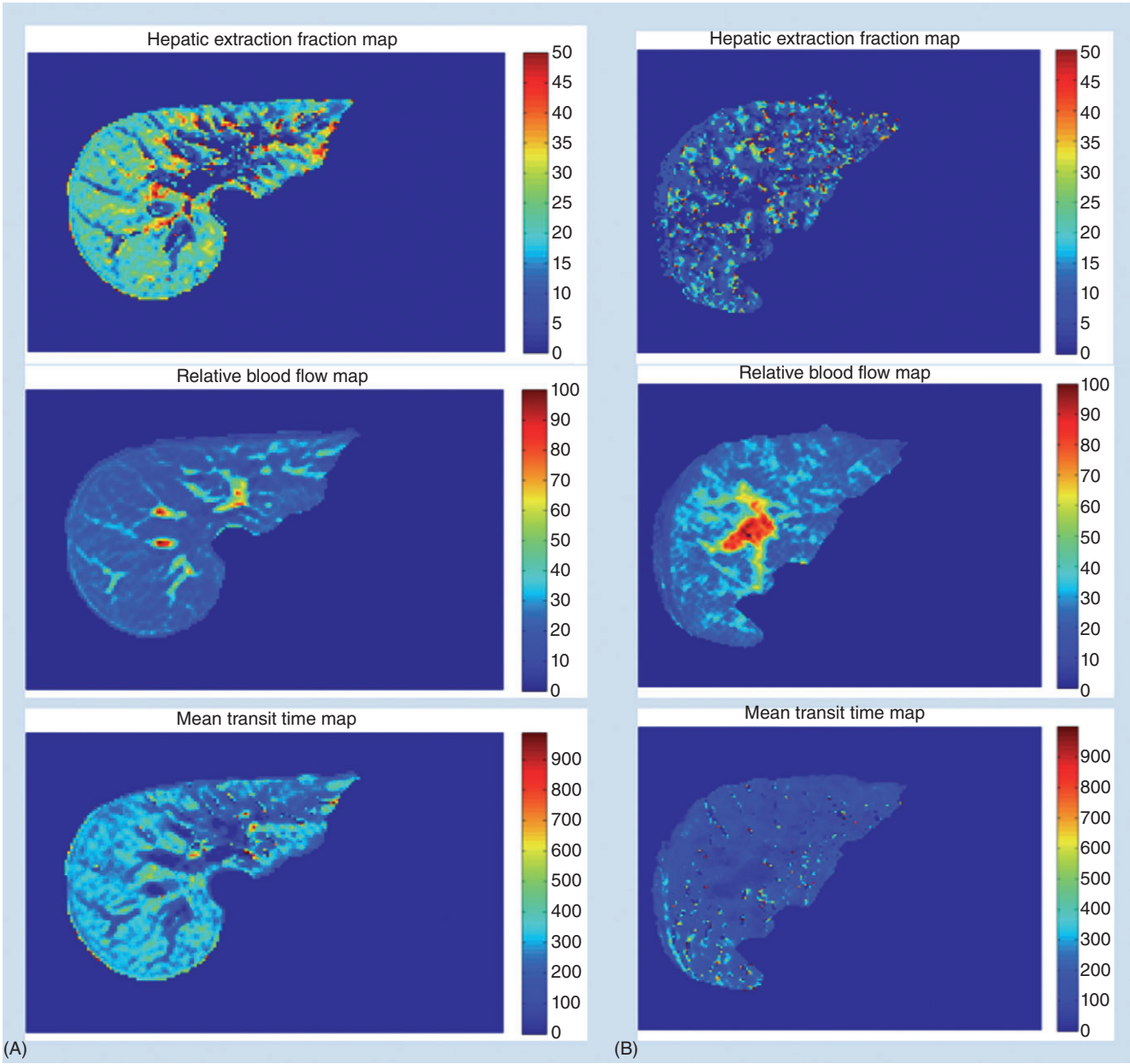

Figure 4 Parametric images of hepatic extraction fraction, input-relative blood flow and mean transit time in one slice of liver calculated for (A) one healthy volunteer and (B) one patient with primary biliary cirrhosis and obvious radiological signs of cirrhosis. All parameters were calculated on a voxel level

The technique described may aid in the management of patients with PBC. Percutaneous liver biopsy still has clinical relevance, although it is not required for definitive diagnosis. DHCE-MRI results can direct biopsies to the most affected parts of the liver, making them more representative. The effect of new therapies can be evaluated by comparing pre- and post-treatment results.

From a surgical perspective, the further development of the method may contribute to better preoperative functional analysis of patients considered for liver resection. Current tests assess global liver function and may fail to detect eventual segmental dysfunction. They may also lead to the inaccurate prediction of postoperative function as they do not account for regional differences in function. As the parametric images in Fig. 4 show, the functional parameters can be derived on a voxel level. If the functional parameter values of all voxels in a segment are added, a quantitative assessment of the functional volume of the segment can be derived. This will enable a much more accurate estimate of

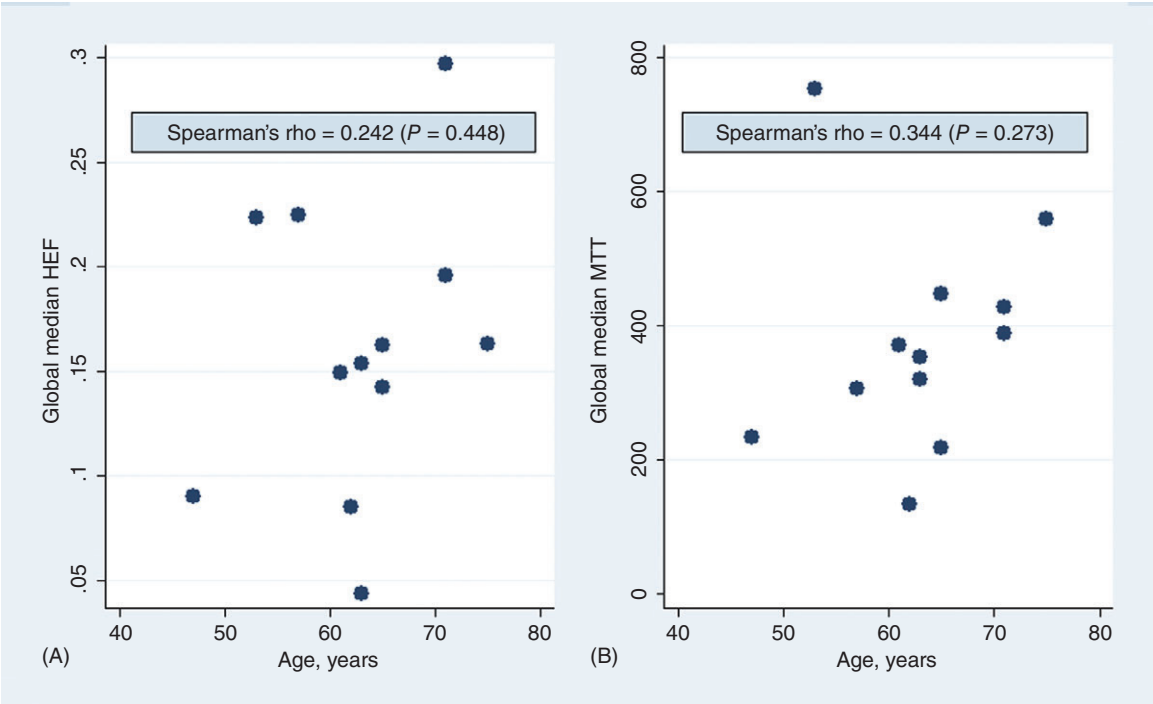

Figure 5 (A) Hepatic extraction fraction (HEF) and (B) mean transit time (MTT) plotted as a function of age in primary biliary cirrhosis patients, showing a weak positive, non-significant correlation

the functional capacity of the future remnant liver in patients undergoing liver surgery.

In summary, this study describes an MRI-based liver function test. In patients with PBC, the model-free parameters can quantitatively assess hepatic function and correlates with disease severity.

Acknowledgements

The authors would like to express their sincere gratitude to Dr Izabella Janczewska, Dr Karin Hagen, Dr Annika Bergquist and R T Tord Jigbrant for their valuable contributions to this project.

Financial support for this study was provided through a regional agreement on medical training and clinical research between Stockholm County Council and the Karolinska Institute, by the Juhlin Foundation, Karolinska Institute and by research grants from the Karolinska Institute.

Conflicts of interest

Dr Blomqvist is a member of Primovist Advisory Board sponsored by Bayer-Schering Pharma AG. There is a patent application registered regarding the method to evaluate hepatocyte function described in this paper. The patent rights are owned by Karolinska Innovations AB, and not by the authors directly.

References

1. Capussotti L, Vigano L, Giuliante F, Ferrero A, Giovannini I, Nuzzo G. (2009) Liver dysfunction and sepsis determine operative mortality after liver resection. *Br J Surg* 96:88–94.
2. Schneider PD. (2004) Preoperative assessment of liver function. *Surg Clin North Am* 84:355–373.
3. Garcea G, Ong SL, Maddern GJ. (2009) Predicting liver failure following major hepatectomy. *Dig Liver Dis* 41:798–806.
4. Aburano T, Taniguchi M, Hisada K, Miyazaki Y, Kakuma K, Fujioka M. (1988) Discordant hepatic uptake of Tc-99m HIDA and Tc-99m colloid in a patient with segmental biliary obstruction. *Clin Nucl Med* 13:599–601.
5. Koizumi K, Uchiyama G, Arai T, Ainoda T, Yoda Y. (1992) A new liver functional study using Tc-99m DTPA-galactosyl human serum albumin: evaluation of the validity of several functional parameters. *Ann Nucl Med* 6:83–87.
6. Torizuka K, Ha-Kawa SK, Kudo M, Kubota Y, Yamamoto K, Itoh K *et al*. (1992) [Phase III multi-centre clinical study on 99mTc-GSA, a new agent for functional imaging of the liver.] *Kaku Igaku* 29:159–181.
7. Schuhmann-Giampieri G. (1993) Liver contrast media for magnetic resonance imaging. Interrelations between pharmacokinetics and imaging. *Invest Radiol* 28:753–761.
8. Hamm B, Staks T, Muhler A, Bollow M, Taupitz M, Frenzel T *et al*. (1995) Phase I clinical evaluation of Gd-EOB-DTPA as a hepatobiliary MR contrast agent: safety, pharmacokinetics, and MR imaging. *Radiology* 195:785–792.
9. Kim T, Murakami T, Hasuike Y, Gotoh M, Kato N, Takahashi M *et al*. (1997) Experimental hepatic dysfunction: evaluation by MRI with Gd-EOB-DTPA. *J Magn Reson Imaging* 7:683–688.
10. Murakami T, Kim T, Gotoh M, Hasuike Y, Kato N, Miyazawa T *et al*. (1998) Experimental hepatic dysfunction: evaluation by MR imaging with Gd-EOB-DTPA. *Acad Radiol* 5 (Suppl. 1):80–82.
11. Ryeom HK, Kim SH, Kim JY, Kim HJ, Lee JM, Chang YM *et al*. (2004)

Quantitative evaluation of liver function with MRI using Gd-EOB-DTPA. *Korean J Radiol* 5:231–239.

12. Schmitz SA, Muhler A, Wagner S, Wolf KJ. (1996) Functional hepatobiliary imaging with gadolinium-EOB-DTPA. A comparison of magnetic resonance imaging and 153gadolinium-EOB-DTPA scintigraphy in rats. *Invest Radiol* 31:154–160.

13. Nilsson H, Nordell A, Vargas R, Douglas L, Jonas E, Blomqvist L. (2009) Assessment of hepatic extraction fraction and input-relative blood flow using dynamic hepatocyte-specific contrast-enhanced MRI. *J Magn Reson Imaging* 29:1323–1331.

14. Crosignani A, Battezzati PM, Invernizzi P, Selmi C, Prina E, Podda M. (2008) Clinical features and management of primary biliary cirrhosis. *World J Gastroenterol* 14:3313–3327.

15. Invernizzi P, Gershwin ME. (2008) The genetic basis of primary biliary cirrhosis: premises, not promises. *Gastroenterology* 135:1044–1047.

16. Invernizzi P, Miozzo M, Battezzati PM, Bianchi I, Grati FR, Simoni G *et al*. (2004) Frequency of monosomy X in women with primary biliary cirrhosis. *Lancet* 363:533–535.

17. Hohenester S, Oude-Elferink RP, Beuers U. (2009) Primary biliary cirrhosis. *Semin Immunopathol* 31:283–307.

18. Scheuer PJ. (1983) Primary biliary cirrhosis: diagnosis, pathology and pathogenesis. *Postgrad Med J* 59 (Suppl. 4):106–115.

19. Christensen E, Neuberger J, Crowe J, Altman DG, Popper H, Portmann B *et al*. (1985) Beneficial effect of azathioprine and prediction of prognosis in primary biliary cirrhosis. Final results of an international trial. *Gastroenterology* 89:1084–1091.

20. Dickson ER, Grambsch PM, Fleming TR, Fisher LD, Langworthy A. (1989) Prognosis in primary biliary cirrhosis: model for decision making. *Hepatology* 10:1–7.

21. Goudie BM, Burt AD, Macfarlane GJ, Boyle P, Gillis CR, MacSween RN *et al*. (1989) Risk factors and prognosis in primary biliary cirrhosis. *Am J Gastroenterol* 84:713–716.

22. Roll J, Boyer JL, Barry D, Klatskin G. (1983) The prognostic importance of clinical and histologic features in asymptomatic and symptomatic primary biliary cirrhosis. *N Engl J Med* 308:1–7.

23. Rydning A, Schrumpf E, Abdelnoor M, Elgjo K, Jenssen E. (1990) Factors of prognostic importance in primary biliary cirrhosis. *Scand J Gastroenterol* 25:119–126.

24. Grambsch PM, Dickson ER, Kaplan M, LeSage G, Fleming TR, Langworthy AL. (1989) Extramural cross-validation of the Mayo primary biliary cirrhosis survival model establishes its generalizability. *Hepatology* 10:846–850.

25. Strasberg SM. (1997) Terminology of liver anatomy and liver resections: coming to grips with hepatic Babel. *J Am Coll Surg* 184:413–434.

26. Strasberg SM. (2005) Nomenclature of hepatic anatomy and resections: a review of the Brisbane 2000 system. *J Hepatobiliary Pancreat Surg* 12:351–355.

27. Dujardin M, Sourbron S, Luypaert R, Verbeelen D, Stadnik T. (2005) Quantification of renal perfusion and function on a voxel-by-voxel basis: a feasibility study. *Magn Reson Med* 54:841–849.

28. Michoux N, Vallee JP, Pechere-Bertschi A, Montet X, Buehler L, Van Beers BE. (2006) Analysis of contrast-enhanced MR images to assess renal function. *MAGMA* 19:167–179.

29. Brown PH, Juni JE, Lieberman DA, Krishnamurthy GT. (1988) Hepatocyte vs. biliary disease: a distinction by deconvolutional analysis of technetium-99m IDA time-activity curves. *J Nucl Med* 29:623–630.

30. Daniel GB, Bahr A, Dykes JA, DeNovo R, Young K, Smith GT. (1996) Hepatic extraction efficiency and excretion rate of technetium-99m-mebrofenin in dogs. *J Nucl Med* 37:1846–1849.

31. Daniel GB, DeNovo R, Bahr A, Smith GT. (2001) Evaluation of heart time-activity curves as a predictor of hepatic extraction of 99mTc-mebrofenin in dogs. *Vet Radiol Ultrasound* 42:162–168.

32. Daniel GB, DeNovo R, Schultze AE, Schmidt D, Smith GT. (1998) Validation of deconvolutional analysis for the measurement of hepatic function in dogs with toxic-induced liver disease. *Vet Radiol Ultrasound* 39:375–383.

33. Doo E, Krishnamurthy GT, Eklem MJ, Gilbert S, Brown PH. (1991) Quantification of hepatobiliary function as an integral part of imaging with technetium-99m-mebrofenin in health and disease. *J Nucl Med* 32: 48–57.

34. Howman-Giles R, Moase A, Gaskin K, Uren R. (1993) Hepatobiliary scintigraphy in a paediatric population: determination of hepatic extraction fraction by deconvolution analysis. *J Nucl Med* 34:214–221.

35. Juni JE, Reichle R. (1990) Measurement of hepatocellular function with deconvolutional analysis: application in the differential diagnosis of acute jaundice. *Radiology* 177:171–175.

36. Rusinek H, Lee VS, Johnson G. (2001) Optimal dose of Gd-DTPA in dynamic MR studies. *Magn Reson Med* 46:312–316.

